Electronic Supplementary Material (ESI) for Journal of Materials Chemistry C

Supplementary Information to;

Structure *vs* properties -chirality, optics and shapes- in amphihilic porphyrin J-aggregates

Zoubir El-Hachemi, Carlos Escudero, Francisco Acosta-Reyes, M. Teresa Casas, Shaul Aloni, Virginia Altoe, Gerard Oncins, Alessandro Sorrenti, Joaquim Crusats, J. Lourdes Campos, Josep M. Ribó*

EXPERIMENTAL *vs* CACULATED DIFFRACTION DATA

h	*k*	*l*	d_{obs} [Å]	d_{calc}[Å]	d*[1/Å]	F(Re)	F(Im)	|F|	Phase[deg]	I/Imax
1	0	3	9.390	9.3707	0.10672	2.0952e+002	9.4575e+000	2.0974e+002	2.58	21.133%
1	0	9	3.250	3.2108	0.31145	-6.0273e-001	9.0555e+001	9.0557e+001	90.38	3.940%
2	0	6	4.670	4.6853	0.21343	-1.1590e+002	-1.7023e+001	1.1714e+002	188.36	6.593%
2	0	8	3.550	3.5691	0.28018	-1.8862e+000	-1.4184e+002	1.4185e+002	269.24	11.974%
3	0	3	7.190	7.1883	0.13912	1.8698e+001	-1.3618e+002	1.3746e+002	277.82	9.078%
3	0	4	6.070	6.0657	0.16486	-3.4061e+001	1.3016e+001	3.6463e+001	159.09	0.639%
6	0	6	3.590	3.5941	0.27823	3.5096e+001	1.2058e+000	3.5117e+001	1.97	0.592%
4	0	6	4.190	4.1928	0.23850	2.0321e+001	-1.0440e+002	1.0636e+002	281.01	5.435%
4	1	4	4.540	4.5371	0.22040	-4.1505e+001	-2.5318e+001	4.8618e+001	211.38	1.136%
5	0	4	4.770	4.7710	0.20960	2.7679e+001	-1.0090e+001	2.9461e+001	339.97	0.417%
7	0	4	3.780	3.7828	0.26435	-8.5232e+000	6.0253e+000	1.0438e+001	144.74	0.052%
8	0	4	3.410	3.4039	0.29378	-2.3116e+001	1.9214e+001	3.0059e+001	140.27	0.538%
0	0	3	9.600	9.5979	0.10419	3.0353e+001	7.2651e+000	3.1210e+001	13.46	0.468%
0	0	4	7.200	7.1984	0.13892	1.3965e+002	1.2997e+001	1.4026e+002	5.32	9.451%
0	0	5	5.250	5.7587	0.17365	-6.0443e+000	2.0431e+001	2.1306e+001	106.48	1.270%
0	0	6	4.790	4.7989	0.20838	-4.8817e+000	6.7149e+001	6.7327e+001	94.16	2.178%
0	0	7	4.110	4.1134	0.24311	4.3925e+001	6.6154e-001	4.3930e+001	0.86	0.927%
0	0	8	3.590	3.5992	0.27784	-5.9194e+001	-6.2388e+000	5.9522e+001	186.02	1.702%
0	0	9	3.190	3.1993	0.31257	1.0092e+001	1.8731e+001	2.1277e+001	61.68	0.217%
0	0	14	2.090	2.0567	0.48622	1.5961e+001	9.2945e+001	9.4305e+001	80.26	5.992%
2	0	0	14.740	14.7450	0.06782	-1.1804e+001	1.9695e+002	1.9730e+002	93.43	18.701%
3	0	0	9.820	9.8300	0.10173	-6.3902e+000	-6.4936e+000	9.1105e+000	225.46	0.040%
4	0	0	7.370	7.3725	0.13564	5.2166e+001	1.4503e+000	5.2186e+001	1.59	1.308%
5	0	0	5.890	5.8980	0.16955	-9.5753e+000	1.4837e+001	1.7658e+001	122.84	0.150%
6	0	0	4.800	4.9150	0.20346	-1.3143e+001	7.9815e+001	8.0890e+001	99.35	3.143%
7	0	0	4.210	4.2128	0.23737	-2.1894e+001	-2.1715e+001	3.0836e+001	224.76	0.457%
8	0	0	3.690	3.6862	0.27128	-9.6487e+001	-2.8468e+001	1.0060e+002	196.44	4.862%

Table S1. The higher differences between observed (d_{obs}) and calculated (d_{calc}) distances is for *h,k,ℓ* (005) (5.25 Å instead 5.75 Å) and *h,k,ℓ* (600) (4.80 Å instead 4.91 Å), both below 10%. F(Re)= Structure Factor (real); F(Im)= Structure Factor (imaginary); |F|= Module; Phase (degree); I/Imax= Intensity %. The *h,k,ℓ* (0014) is only observed by the electron diffraction microscopy (Barcelona and Berkeley); *h,k,ℓ* (504) was more intense due to intra- and inter-layer disorder: *h,k,ℓ* (700) was more intense due to intra-layer disorder and also because of overlapping with (021).

Diffraction data cif file (FINAL-ribo-SDF2.cif) is attached as additional material for reviewing.

Relative configuration of the building blocks units in the dimers mosaic of the architecture on the plane [$\bar{1}01$]

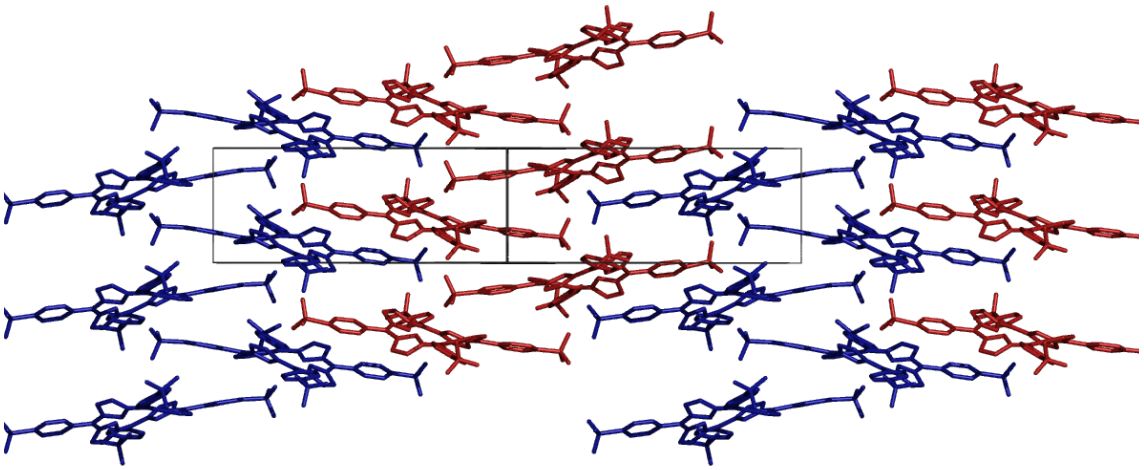

Fig. S1. Image (detail of Fig. 3) of the porphyrin architecture on the plane [$\bar{1}01$] showing the configurations of the porphyrin building blocks [locked conformational enantiomerism; *P* (blue) and *M* (red), see note[26] in the principal text for the definition used to describe the configuration of the porphyrin building blocks).

LD of oriented H_4TPPS_4 J-aggregates

A drop of J-aggregate solution was flowed along an oriented polyamide support and dried. Optical polarization properties were determined from the experimental Mueller matrix obtained by a 2-photomodulators polarimetry as previously described.[7b,c] 0° and 90° correspond respectively to the alignment of the substrate orientation parallel and perpendicular to the polarization measurement.

Fig. S2 corresponds to the correct interpretation of the previous reported results.[27] This error had arised because of the wrong assignment of the polarization of the light beam. According to the correct definition of parallel polarization (parallel to the laboratory roof) the 0° of the figure corresponds approximately to the H-band aligned along the long axis of the particles and the J-band perpendicular to it. This is in agreement with the X-ray and electron diffraction data presented here.

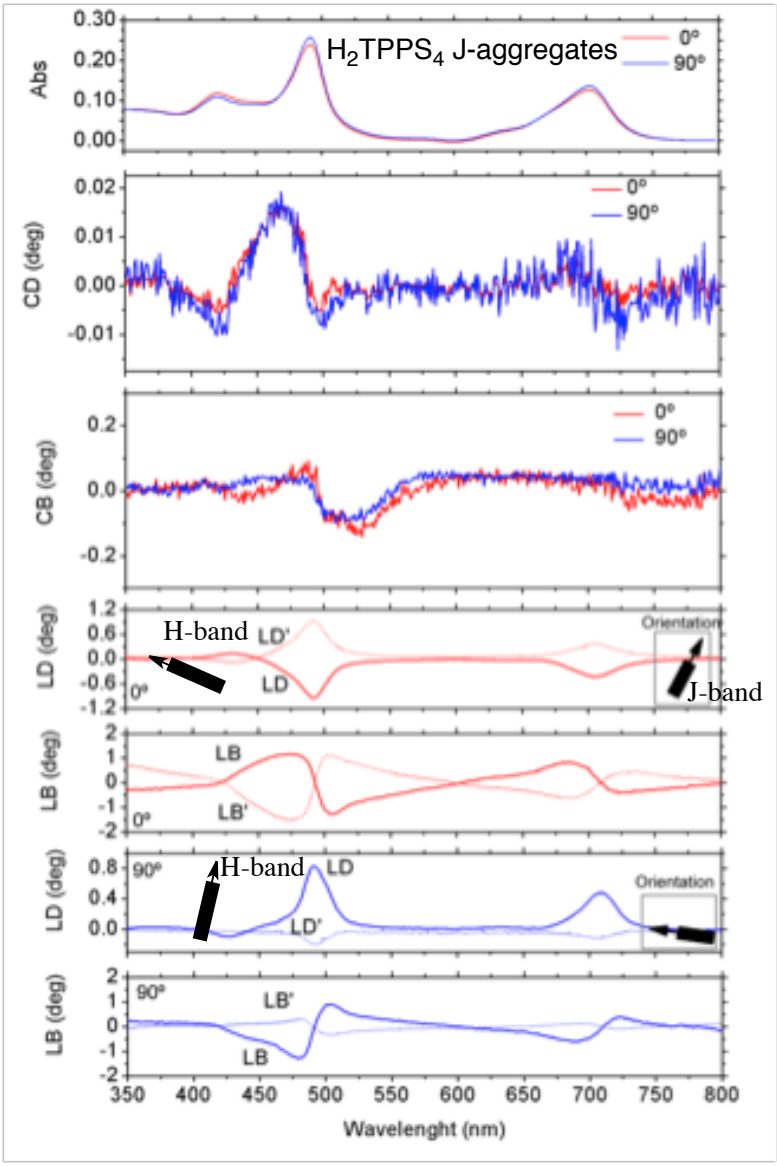

Fig. S2. Optical polarization properties of aligned H_4TPPS_4.

Resonance Light Scattering (RSL) of $H_4TPPF_5S_3$ J-aggregates showing the presence of oligomers

The $H_4TPPF_5S_3$ J-aggregates at the first stages of aggregation can show, depending on the experimental conditions, red shifted absorptions corresponding to side-to-side oligomers.[10] For details on the preparation of the samples of Fig. S4 see ref.[10].

Fig. S3 shows how these oligomeric absorption bands yield RLS bands; a) the low absorbance values exclude the presence of auto-absorption phenomenon: b) the ≈ 5 nm red shift of the RLS band, with respect to the absorption band, is characteristic of this type of J-aggregates.[S1] The presence of RLS for these absorption bands implies that the oligomeric absorption is forming a big set of chromophores, for example like those of the sheet of the Fig. 5 of the principal text.

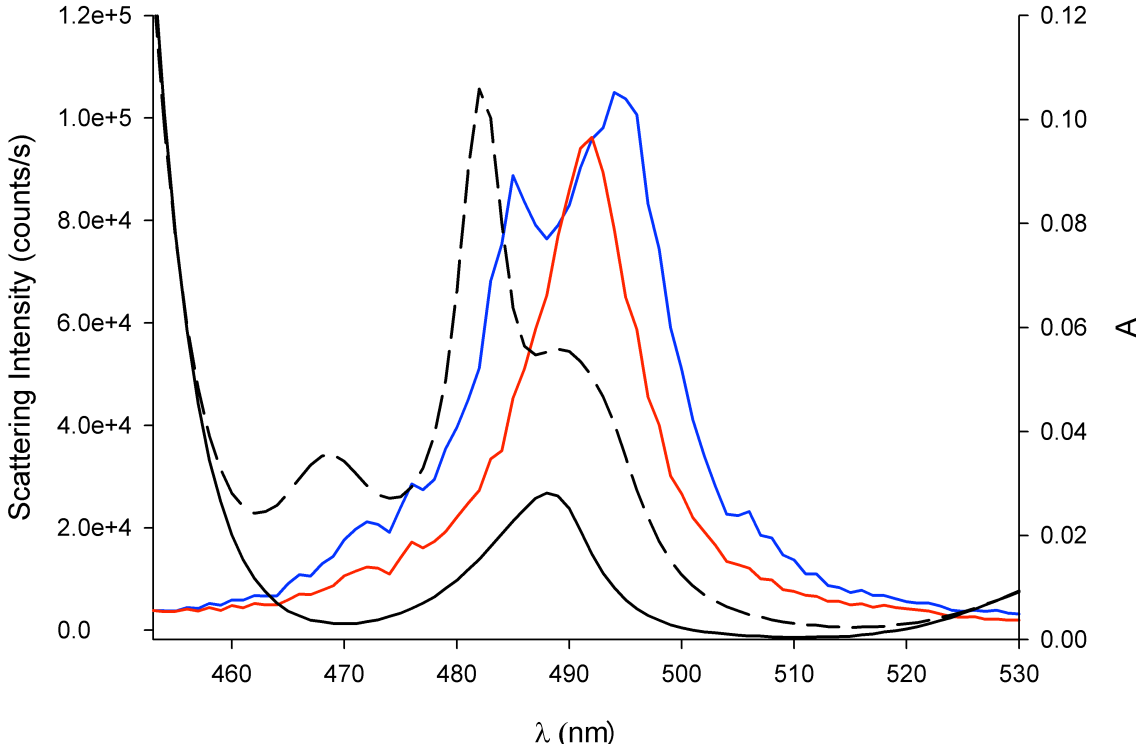

Fig. S3. RLS and UV/Vis absorption spectra at the first stages of the $H_4TPPF_5S_3$ aggregation. *UV/Vis absorption spectra:* Solid black line (peak maxima; 468 nm, 482 nm, and band from the addition of 488 nm + 492 nm) and dashed line (peak maxima; 488 nm); both spectra correspond to samples containing different aggregated species and stereoisomers.[10] *RLS spectra:* Red line corresponds to the RLS spectrum (493 nm) of the sample with the solid black absorption spectra; blue line corresponds to the RLS spectrum (472 nm, 485 nm, 492 nm and 496 nm) of the sample with the dashed black absorption spectrum.

S1. Collings, P. J.; Gibbs, E. J.; Starr, T. E.; Vafek, O.; Yee, C.; Pomerance, L.A.; Pasternack, R. F. *J. Phys. Chem. B* **1999**, *103*, 8474-8481.

TEM (BERKELEY)

In Fig. S4 we show the sequence of data acquired in a regular experiment. First the sample was imaged in TEM mode to get an overall idea of the structures present. After that we switched to STEM mode moving to a new area of the sample (to avoid artifacts due to beam damage inflicted to the sample area exposed to TEM measurements). By using the low-resolution parallel beam we got a low-resolution image of the sample (≤ 3μs/pixel dwell times, Fig. S4A) and the sample area of interest is selected with the digiscan software controls. The area selected is scanned using the Gatan's scanning electronics obtaining at the same time a low-resolution HAADF STEM image and the diffraction patterns pixel by pixel. The typical acquisition area was 1 μm x 1 μm or 2 μm x 2 μm with a step size of 100 nm, 0.4 sec/pixel and a camera exposure of 0.2 sec. After that, the convergent beam was used to get a high resolution HAADF STEM image with a 0.2 sec/pixel rate of the area scanned with the parallel beam using the same magnification in both modes. To analyze the data the diffraction patterns were superimposed with the high resolution HAADF STEM image to correlate the different diffraction patterns to specific structures in the area of the sample studied. The electron dose was controlled as detailed in ref.[21] to minimize sample exposure and avoid electron beam damage

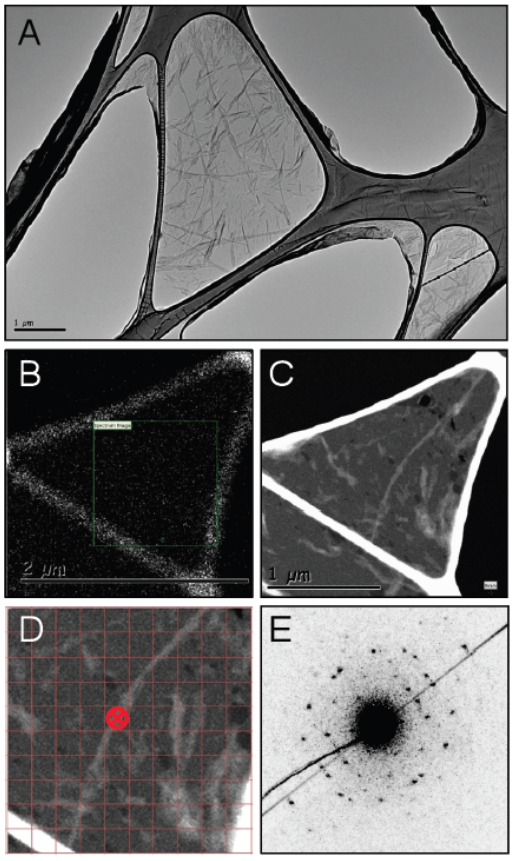

Figure S4. TEM images and STEM diffraction images acquired in a regular experiment to study H_4TPPS_4 aggregates on an ultrathin lacey carbon film. (A) TEM image showing the H_4TPPS_4 homoassociates structures as long-tapes (2kX magnification) on a monolayer of the same porphyrin; (B) survey image (2 μm x 2 μm) using a low-resolution parallel probe. A green square shows the sample area selected to scan and get simultaneously a low resolution HAADF STEM image and diffraction patterns pixel by pixel. (C) When finishing the acquisition of the diffraction patterns, a high-resolution HAADF STEM image (2 μm x 2 μm) is acquired. (D) The overlap of this image and the electron diffraction patterns (14.5° CW rotation of ED with respect to acquiered image; see Material and Methods) allows the correlation of the latter with the specific structures of the sample. For example the diffraction pattern shown in (E) corresponds to the area marked with a crossed red circle in (D).

Thickness of H_4TPPS_4 J-aggregate particles as determined by AFM

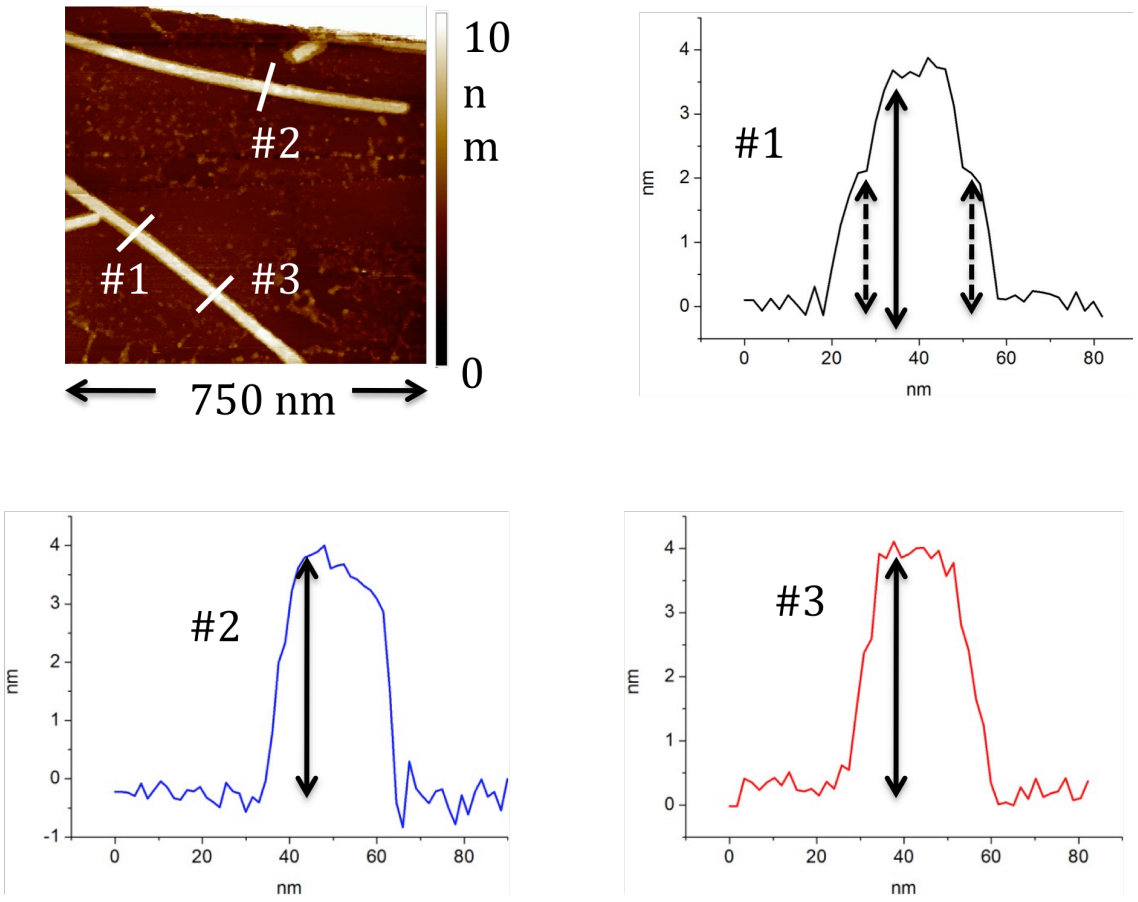

Fig. S5. AFM image of H_4TPPS_4 J-aggregate particles. The thickness corresponds to 3.85 nm ± 0.15 nm. In some cases the thickness of the monolayer at the edges of the particle could be observed (for example in section #1). The average thickness was 3.85 ± 0.15 nm for the bilayer and 1.85 ± 0.5 nm for the monolayer. These thicknesses correspond to those expected from the diffraction data (see text) for mono and bilayers.